A Geometric Approach to Passive Target Localization

S. Wong, R. Jassemi-Zargani, D. Brookes, and B. Kim
3701 Carling Ave., Ottawa, Ontario, K1A 0Z4
CANADA

silvester.wong@drdc-rddc.gc.ca rahim.jassemi@drdc-rddc.gc.ca dan.brookes@drdc-rddc.gc.ca
bumsoo.kim@drdc-rddc.gc.ca

ABSTRACT

Passive detection offers a viable and effective means for geolocating small flying targets such as micro- and nano-drones by exploiting their radio-frequency signal emissions. Target localization using the Time-Difference-Of-Arrival (TDOA) method is investigated. A geometric approach to solving the TDOA problem is examined in this study. For target localization in 3-dimensional space, a set of 3 non-linear TDOA equations is required. Each equation contains a TDOA measurement processed from signals detected by a pair of receivers. A system of 4 receivers is used to generate 3 independent TDOA measurements. The solution to each TDOA equation is represented by a hyperboloid surface. The intersection of 3 hyperboloid surfaces is then computed to determine the target location in 3-dimensional space.

The target localization problem is analyzed by examining the effect of TDOA measurement errors on the localization accuracy. The errors are modelled by the Cramer-Rao Lower Bound (CRLB) variance in processing the signals through a cross-correlator. Results indicate that the TDOA measurement errors have a notable effect on the accuracy of the target locations.

Localization of multiple targets is also investigated. Accurate localization results for up to 7 moving targets have been obtained by applying the geometric approach. A discussion on how the geometric approach could be exploited for real-time multi-target localization is given. This will potentially offer a practical tool in defence and security applications.

1.0 INTRODUCTION

Mini-drones and micro-drones are seen as technologies that are increasingly posing security threats to military operations, public security, and national interests. These threats include military scouting and targeting reconnaissance by adversaries against Arctic expeditionary force operations, potential drone-airplane collisions near airport/airfield runways, security breaches around nuclear power plants, intrusions to sensitive government infrastructures, and natural resources prospecting in the Arctic by private multi-national corporations. A proliferation of these flying machines is expected to inundate the airspace in the not too distant future; thus a capability to detect and track these targets is foreseen to be a useful asset and will be in demands in the defence and security domains.

Detecting small drone targets can be quite challenging for conventional methods such as active-radars and EO/IR sensors because of their small size, low-thermal emission characteristics, and low radar cross-section due to size and construction materials. On the other hand, passive detection methods can be quite useful for detecting small drones. For example, radio-frequency (RF) emissions from drones such as First-Person-View

remote piloting, image data transmissions and telemetry communication can readily be exploited for passive detection and tracking.
A well-established method used in passive target location of non-cooperative targets exploiting the target's own radio-frequency emissions is the TDOA measurement technique [1, 2]. It deploys a number of time-synchronized sensors to produce a fix on the target's location.

TDOA methods have been researched and developed extensively for more than 4 decades [3]. The majority of the TDOA signal processing algorithms reported in the literature are based on the algebraic approach in solving a set of 3 non-linear hyperbolic equations [4,5,6]. Essentially, these equations are solved by numerical iterative methods to locate the target. There are a number of variations on the techniques developed for the algebraic approach, iterative statistical methods [2,6,7,8] and closed-form algebraic solutions [4,9,10,11]. However, when the TDOA measurements from the sensors have sizable errors, the closed-form algebraic solution will have poor target localization accuracy. Iterative techniques must then be applied to optimize the solution. Iterative numerical processing can be computationally intensive; thus it is a challenge to apply it to real-time applications.

As drones are becoming more affordable and more accessible, future target detection system will likely require a multi-target localization capability to counter the practice of multiple-drones missions. There are only a few reported works in the literature on multi targets localization, for example [7,8,12]. They are analyzed via iterative numerical methods which are computational intensive, making multiple-targets processing unlikely to be real-time.

An alternative approach to solving the TDOA problem is exploring the geometric approach in solving the set of nonlinear hyperbolic equations. This method relies on finding the intersection of 3 hyperboloids as the target location. There have been a number of investigations on the geometric approach [3,5,11,13]. It is shown that a simple numerical procedure can be used to determine the intersecting location of 3 hyperboloids, and target location can be determined accurately.

It will also be shown that multi-target localization can be obtained accurately in a relatively simple manner. The geometric approach enables hyperboloids to be pre-computed for a set of possible TDOA measurement values for a given detection system configuration, and look-up tables for a set of hyperboloids can then be compiled. This speeds up the process of target localization considerably and opens up a potential means for real-time multiple targets localization to be realized.

The objective of this paper is to present a technical framework of the TDOA method and procedures based on the geometric approach for finding target locations. Results will be presented and discussed to show that multi-target localization can be achieved accurately.

2.0 TARGET LOCALIZATION USING THE TDOA METHOD

2.1 TDOA for target localization

The TDOA method is based on the principle of locating a target along a 3-dimensional geometrical surface where the time difference of arrival of a target signal between a pair of synchronized receivers is constant. This surface is described by a hyperboloid. Using a set of 4 receivers, 3 independent TDOA measurements can be made [4]. The TDOA measurements are then converted to hyperboloid surfaces. The intersecting point formed by the 3 hyperboloids determines the target's location in 3-dimensional space.

In order to provide a clear illustration of how TDOA measurements can be made, a typical ground receiver configuration is used for illustration; this is shown in Figure 2.1. There are 4 receivers (S1, S2, S3, S4) in the passive detection system unit. The system in Figure 2.1 is configured in a "forward looking" mode such that the receivers are monitoring the airspace at the top of Figure 2.1a (yellow shaded area). Furthermore, the receivers are assumed to have a wide field of view in azimuth and elevation so that all 4 receivers monitor the same volume of airspace at the same time in staring-mode. The dimensions of the area-of-interest monitored by the system shown in Figure 2.1 correspond to an area coverage in a typical small drone detection scenario where the drone is emitting 500 mW of power from its First Person View transmitter.

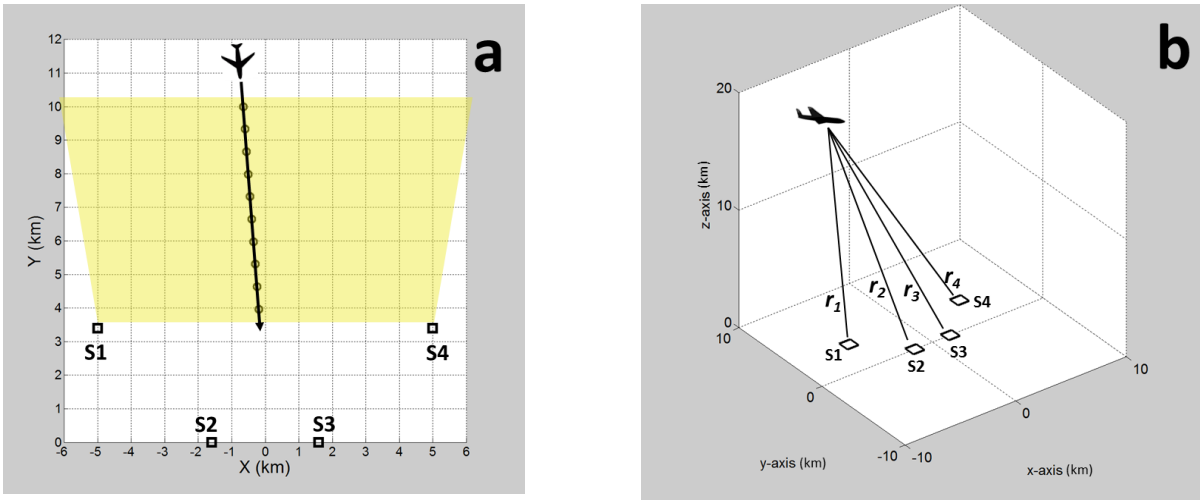

Figure 2.1: Passive target detection system configuration; a) plan view, b) 3-dimensional view.

2.2 TDOA equations

Three time-synchronized coherent receiver pairs, S1-S2, S3-S4 and S1-S4 are formed from the set of 4 receivers in Figure 2.1 to collect 3 independent sets of TDOA measurement data. For example, TDOA τ_{12} is measured by receiver pair S1-S2, TDOA τ_{34} by S3-S4 and TDOA τ_{14} is measured by S1-S4. Time synchronization between receivers can be achieved readily using GPS-disciplined oscillators. Details on how the TDOA measurements are made will be discussed later in Section 3. It is sufficed to say that 3 independent TDOA measurements are needed to detect and to locate a target. The set of 3 TDOA equations are,

$$\begin{aligned} d_{12} &= c\tau_{12} = r_1 - r_2 \\ d_{34} &= c\tau_{34} = r_3 - r_4 \\ d_{14} &= c\tau_{14} = r_1 - r_4 \end{aligned} \tag{2.1}$$

where $d_{ij} = c\tau_{ij}$ is the range-difference (i.e., TDOA measurements expressed in length unit) of the target relative to receiver i and receiver j, c is the speed of light, and $r_i = ((x - X_i)^2 + (y - Y_i)^2 + (z - Z_i)^2)^{1/2}$ is the L_2-norm (Euclidean) distance between the target (x,y,z) and receiver (X_i, Y_i, Z_i), $i = 1,2,3,4$ (see Figure 2.1b). For simplicity and consistency, d_{ij} will be referred to as the "TDOA measurement". Each of the equations in Equation (2.1) represents a 3-dimensional hyperboloid surface geometrically; this will be discussed in more details in Section 2.3. Since the receiver positions (X_i, Y_i, Z_i) are known and the TDOA measurement values d_{ij} can be made, Equation (2.1) with 3 independent equations can hence be solved for the 3 unknown target variables (x,y,z) to find the target location. Target localization will be conducted using a geometric approach.

This approach offers a simple algorithm that is also applicable to multi-target localization, and has the potential for real-time multi-target processing.

2.3 Geometric approach

The geometric approach used here is a geometry-based method to generate 3 hyperboloids from the 3 equations in Equation (2.1); it then looks for the intersecting point among the 3 hyperboloids as the target location. Geometrically, Equation (2.1) describes 3 intersecting hyperbolic surfaces. It will be shown that in the ideal case when there is no TDOA measurement error in the d_{ij}, the 3 hyperboloids do intersect at a point; this will be presented in the analysis in Section 4. However in practice, the TDOA measurements will always contain errors due to system noise and target signal characteristics such as bandwidth; only an estimate of the target location can be made. The localization accuracy is thus subject to the size of the TDOA measurement error.

Mathematically, the geometric form of each hyperboloid in Equation (2.1) can be more simply described by considering each pair of receivers in its own local coordinate frame of reference. This is to distinguish it from the common coordinate frame in which all the receivers and targets must reside in order to determine the target location; this common frame shall be called the global coordinate frame.

Receiver pair S1-S2 will be is used as an illustrative example. In the local frame, the receiver pair separated by a distance d is placed on the x'-axis symmetrically. That is to say, receiver S1 has the coordinate $(X',Y',Z')_1 = (-d/2,0,0)$, and receiver S2 has the coordinate $(X',Y',Z')_2 = (d/2,0,0)$. Furthermore, the y' axis is oriented such that the target is situated in the x'-y' plane; i.e., with coordinates (x',y'). Thus, a local frame is defined in which the 2 receivers and a target are all confined in a 2-dimensional plane (i.e. x'-y' plane). This is illustrated schematically in Figure 2.2.

Using the first equation in Equation (2.1) for the S1-S2 pair, and substitute in the receivers and target coordinates,

$$\begin{aligned} d_{12} &= r_1 - r_2 \\ &= \sqrt{(x'-X_1')^2 + (y'-Y_1')^2} - \sqrt{(x'-X_2')^2 + (y'-Y_2')^2} \\ &= \sqrt{\left(x'+\frac{d}{2}\right)^2 + y'^2} - \sqrt{\left(x'-\text{—}\right) + y'} \end{aligned} \qquad (2.2)$$

After some algebraic rearrangements, Equation (2.2) can be re-expressed as,

$$\frac{x'^2}{\left(\frac{d_{12}^2}{4}\right)} - \frac{y'^2}{\left(\frac{d^2}{4} - \frac{d_{12}^2}{4}\right)} = 1 \qquad (2.3)$$

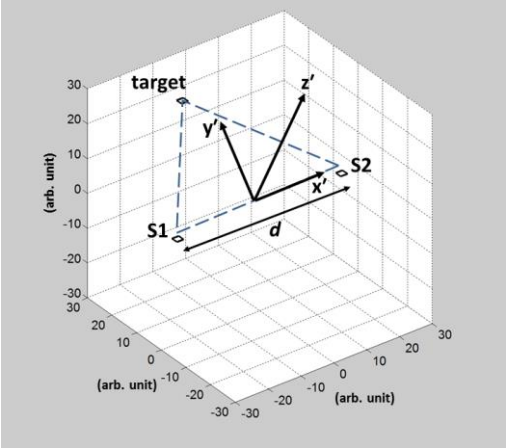

Figure 2.2: A pair of receivers (S1-S2) and a target are situated in local coordinate frame.

Equation (2.3) is a 2-dimensional "hyperbola of 2-sheet" [14]. A 3-dimensional hyperboloid can be generated by the method of volume of revolution about the x′-axis. The hyperboloid is thus given by,

$$\frac{x'^2}{a^2} - \left(\frac{y'^2}{b^2} + \frac{z'^2}{b^2} \right) = 1 \qquad (2.4)$$

where $a = (d_{12}/2)$, $b = (d^2 - d_{12}^2)^{1/2}/2$, $d > d_{12}$. Physically, the hyperboloid surface represents an isochrone where a point anywhere on the surface has the same time difference of arrival (TDOA) with respect to receivers S1 and S2. Recasting Equation (2.4) in the form,

$$x' = \pm \left| \left| 1 + \left| \frac{y'^2}{b^2} + \frac{z'^2}{b^2} \right| \right| \right|^{1/2} \qquad (2.5)$$

It can be seen that there are 2 distinct hyperboloid surfaces that can exist; one has $+|a|$ value and the other has $-|a|$ value in Equation (2.5). These 2 hyperboloids are shown in Figure 2.3. Moreover, because the hyperboloid is a surface generated from volume of revolution about the x'-axis, it is symmetrical azimuthally in the y'-z' plane (i.e., circle) as indicated in Equation (2.5). Thus, the local frame axes can be redefined, with the z'-axis as pointing vertically upward as illustrated in Figure 2.3.

Recall from Equation (2.4) that the parameter a, is effectively the TDOA measurement value d_{12}. The TDOA measurement value can take on either positive or negative value; this can be clearly seen from Equation (2.2). If the target is closer to receiver S2 than to receiver S1, then a is positive because $d_{12} = r_1 - r_2$ is positive; otherwise, a is negative. When the target is exactly the same distance from both receivers (i.e., $a = 0$), Equation (2.5) degenerates into a plane described by $x' = 0$.

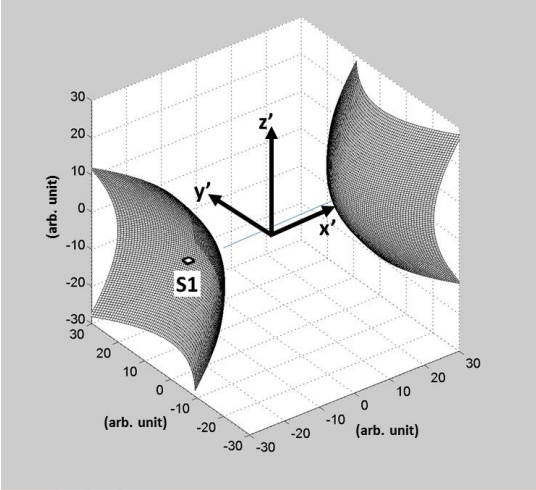

Figure 2.3: Orientation of the hyperboloids in local coordinate frame (x′,y′,z′) in 3D.

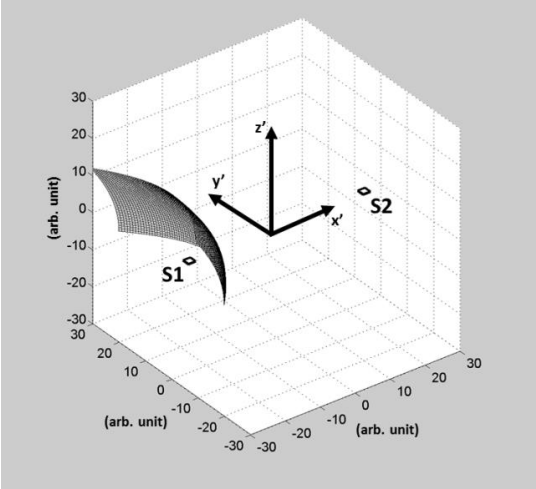

Figure 2.4: A hyperboloid representing the TDOA of an air target as detected by a pair of receivers in local coordinate frame.

The TDOA measurement d_{12} of a target will have either a plus or minus sign associated with it. Therefore, only one of the two hyperboloids in Figure 2.3 is valid. If the TDOA measurement value d_{12} is negative (i.e., $r_1 < r_2$), only the hyperboloid closer to receiver S1 is valid. Furthermore, for an air surveillance scenario, only the upper half of the hyperboloid is relevant ($z' \geq 0$); this is shown in Figure 2.4. Thus the geometric solution automatically constrains the solution to the correct sector of the airspace volume. In effect, the hyperboloid surface shown in Figure 2.4 represents the solution to the first TDOA equation in Equation (2.1). Hyperboloids for receiver pairs S3-S4 and S1-S4 can be obtained in the exact same manner in their own local coordinate frame (x',y',z').

2.4 Putting the hyperboloids in common global coordinate frame

To solve the TDOA equations in equation (2.1) for locating a target, the 3 hyperboloids must be mapped onto a common global coordinate frame (x,y,z) and properly oriented relative to their respective receiver pairs so

that the intersection of the 3 hyperboloid can be determined. For the system configuration of the 4 receivers shown in Figure 2.1, the hyperboloids from their own local frames can be mapped onto a common global frame through a series of translations and rotations. As illustration, a coplanar system configuration in which the 4 receivers are situated on the same plane (z=0) is used. The receiver pairs (S1-S2, S3-S4, S1-S4) and their associated hyperboloids are moved from their respective local frames to a common frame.

Using receiver pair S1-S2 as an illustrative example, the procedure for mapping a hyperboloid from its local frame (x',y',z') to the global frame (x,y,z) is performed as follows. First, the x'-z' axes at y'=0 of the local frame is overlaid parallel to the x-z axes at y=0 of the global frame. This effectively overlays (x',y',z') onto (x,y,z). The task is then to map receiver-pair S1-S2 and its associated hyperboloid from the local coordinate position (Figure 2.4) to its proper location in the global coordinate frame (Figure 2.1b), conforming to the receiver system configuration. That is to say, since the hyperboloid is fixed in position relative to receivers S1 and S2, the hyperboloid will move in the exact same manner as the 2 receivers from the locations in local coordinate frame to locations in the common global coordinate frame.

To begin the mapping process, the receiver-pair (S1-S2) and its associated hyperboloid as an ensemble (referred to as the "ensemble" hereafter) is first translated such that S2 at (d/2,0,0) is moved to (x,y,z) = (0,0,0); i.e.,

$$\begin{aligned} {}_{new1} &= x_{old} \quad \frac{d}{2} \\ y_{new1} &= \quad {}_{old} \\ z_{new1} &= \quad {}_{old} \end{aligned} \tag{2.6}$$

Receiver S2 is then acted as the pivot to rotate the ensemble about the z-axis. A rotation in the clockwise direction by an angle,

$$\phi = \arctan\left(\frac{Y_1 - Y}{X_1 -}\right) \tag{2.7}$$

is performed, where (X_i,Y_i,Z_i), i=1,2 are the ground-truth locations of receivers S1 and S2 in the global frame. The clockwise-rotated coordinates of the ensemble are given by,

$$\begin{aligned} x_{new2} &= x_{new1}\cos(-\phi) - y_{new1}\sin(- \ ) \\ y_{new2} &= x_{new1}\sin(-\phi) + y_{new1}\cos(- \ ) \end{aligned} \tag{2.8}$$

This provides the proper orientation of the receiver pair S1-S2 with respect to the x-axis in the x-y plane. The final position of the ensemble is arrived at through a translation,

$$\begin{aligned} x_{final} &= x_{new2} \quad X \\ y_{final} &= y_{new2} \quad Y \\ z_{final} &= z_{new2} \quad Z \end{aligned} \tag{2.9}$$

The same procedure above is applied to receiver pair S3-S4 to put its associated hyperboloid in the global coordinate frame. S3 is first translated to (x,y,z) = (0,0,0) to serve as a rotating pivot. The receivers-hyperboloid ensemble is rotated counter-clockwise by an amount ϕ, and then translated to the final position relative to the ground truth location of S3, (X_3 ,Y_3 ,Z_3). For the third receiver pair (S1-S4) and its corresponding hyperboloid, the final positions are obtained simply by a translation in the positive y-axis direction by an amount Y_1. Example of 3 hyperboloids in a common coordinate frame intersecting with one another is illustrated in Figure 2.5. For system configuration with a non-coplanar geometry in which receivers

can be situated at different heights z, the mapping from the local frames to a common frame is a bit more complex; this is discussed in [15].

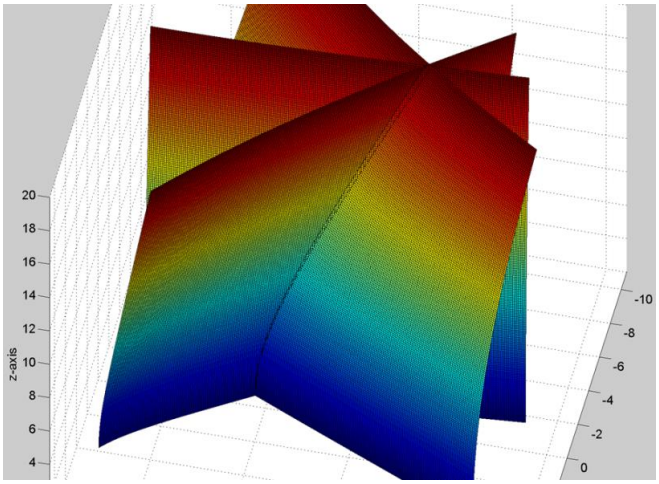

Figure 2.5: 3 intersecting hyperboloids in a common global coordinate frame.

3.0 TDOA MEASUREMENTS

3.1 cross-correlation processing

TDOA measurements (d_{ij}) are obtained from the signals, detected by a pair of receivers i and j, processing processed through a cross-correlation process [16,17,18]. A brief description is summarized as follows. First, signals from a pair of receivers (Si-Sj) are processed using the cross-ambiguity function [19],

$$\chi(\tau_i', \tau_j') = \int \eta_i(t-\tau_i')\eta_j^*(t-\tau_j')\,dt \tag{3.1}$$

where

$$\begin{aligned} \tau_i' &= \tau + \frac{f_{D,i}t}{f} \\ \tau_j' &= \tau + \frac{f_{D,j}t}{f} \end{aligned} \tag{3.2}$$

τ_i and τ_j are the signal arrival times from the target to receivers i and j respectively; $f_{D,i}$ and $f_{D,j}$ are the line-of-sight Doppler frequencies as seen between the target and receivers i and j respectively. t and f are the time and frequency variables. Let $t' = t - \tau_1'$, then $t = t' + \tau_1'$; thus $t - \tau_2' = t' - (\tau_2' - \tau_1')$, and $dt' = dt$. Equation (3.1) can be rewritten as,

$$\chi(\tau, f_D) = \int \eta_i(t)\eta_j^*(t-(\tau_j' - \tau_i'))\,dt \tag{3.3}$$

where

$$(\tau_j' - \tau_i') = (\tau_j - \tau_i) + (f_{D,j} - f_{D,i})\frac{t}{f} = \tau + \frac{f_D}{f}t \tag{3.4}$$

and $\tau = (\tau_j - \tau_i)$ is the time difference of arrival (TDOA), and $f_D = (f_{D,j} - f_{D,i})$ is the frequency difference of arrival (FDOA). Equation (3.3) is in the conventional form of the matched filter response function. The terms

matched filter and ambiguity function are sometimes used interchangeably [20]. Mathematically, Equation (3.3) is a cross-correlation process.

It is well recognized that the matched filter process can be performed more efficiently in the frequency domain by making use of the relation [20,21],

$$\chi(\tau, f_D) = \int \eta_i(t')\eta_j^*(t' - (\tau_j' - \tau_i'))\,dt' = \int_\beta U_i(f)U_j^*(f)\exp(j2\pi f(\tau_j' - \tau_i'))df \quad (3.5)$$

That is to say, the matched filtering process can be performed simply by a straight-forward multiplication operation of the spectral signal $U(f)$ in the frequency domain over the signal bandwidth β, instead of a correlation in the time domain.

In dealing with measured data, the spectral signals extracted from a temporal segment of a data leg are in the form of in-phase and quadrature (I,Q) signals in the frequency domain. The output from the cross correlator can be expressed as [15],

$$H_i \quad \int_\beta U_i(f)U_j^*(f)\exp(j2\pi f(\tau_2' - \tau_1))df = \sum_{n=0}^{N-1}\left[(I,Q)_n\right]\exp\left(j\frac{2\pi}{N}ni\right) \quad (3.6)$$

Note that Equation (3.6) implies that the time-domain matched filter process is a Fourier transform of the receiver signals in the frequency domain. H is a function that contains τ (TDOA) and f_D (FDOA) information as defined in Equation (3.4). Physically, the envelope of H can be interpreted as a 1-dimensional target range profile (in SAR terminology) located along the range-difference ($c\tau$) axis somewhere between the 2 receivers that are deployed to produce the cross-correlation signal. Index i is the range-difference bin number of the target signal profile envelope $|H|$; i.e., i = 1, 2, …, N. The location of the peak of $|H|$ is the TDOA measurement value d_{ij} sought in the TDOA equations. Target location is then obtained by solving the set of TDOA equations in Equation (2.1).

3.2 TDOA measurement errors

The TDOA measurements (d_{ij}) will have errors introduced; the errors will affect the accuracy of target localization [9,13,14]. The errors can be described statistically by the Cramer-Rao Lower Bound variance [17,22,23],

$$\sigma \geq 2\frac{E}{N_0}B^2\Bigg)^{-1} \quad (3.7)$$

where E is the signal energy [J], N_0 is the noise spectral power density [W/Hz], and B [Hz] is a width measure of the signal bandwidth, $B = \pi\beta/(3^{1/2})$ [17]. It can be seen that the errors are dependent on the signal and noise levels and the signal's bandwidth. To analyze the signal and noise effect, zero-mean white Gaussian noise can be added to the signals in Equation (3.24) [17,18,22]; i.e.,

$$\eta_i(t) = u_i(t) + n_i(t) \quad (3.8)$$

where $u(t)$ is the signal, $n(t)$ is the additive white Gaussian noise, subscript i denotes the i-*th* receiver in the detection system.

The expression for the Cramer-Rao Lower Bound for the TDOA measurement error has been given in different forms from various analyses in the literature; it has been shown that all these different expressions can be re-expressed in a common form [23]. This form of the Cramer-Rao Lower Bound error is given as [16],

$$\sigma \geq \frac{1}{\beta\sqrt{(2\pi^2/3)\beta_n T(S/N)}} = \frac{1}{\beta\sqrt{6.5\,(S/N)_T}} \tag{3.9}$$

where $T = E/S$ is the signal integration time [s], S is the signal power [W], β_n is the receiver noise bandwidth [Hz], and $N = N_0\beta_n$ is the noise power [W]; note that σ has units in seconds [s]. S/N is the input signal-to-noise ratio (SNR) to the cross correlator. The factor $(S/N)_T = \beta_n T(S/N)$ in the denominator in Equation (3.32) can be thought of as the time-integrated output SNR of the correlated signal processed through the cross-correlator.
From Equation (3.9), the estimated TDOA measurement error ε in spatial units, metres [m] can be rewritten as,

$$= c\sigma \geq \frac{c}{\beta\sqrt{6.5(S/N)_T}} \tag{3.10}$$

where c is the speed of light. Using Equation (3.10), the amount of TDOA measurement with error (d_{ij}) can be modelled by inputting the bandwidth β and the cross-correlator SNR $(S/N)_T$ information into the Fourier transform process in Equation (3.6) that generates the range-difference signal envelope $|H|$.

The accuracy of the signal profile peak's location (i.e., d_{ij} value) is determined by the ability of how close the resolution cell graduated marker with spacing $\Delta r = c/\beta$ can be assigned to the signals, and the spacing within a resolution cell Δr can be further sub-divided into smaller graduation (i.e., finer granularity) by inserting extra bins through the zero-padding process in the Fourier transform to reflect the SNR [15]. This translates to location error of the signal profile peak $|H|$ based on how fine the peak can be measured along the range-difference axis. In brief, TDOA measurements with errors can be estimated statistically in a quantitative manner by applying the Cramer-Rao Lower Bound parameters, β and SNR $(S/N)_T$, in the cross-correlation.

4.0 APPLYING THE GEOMETRIC APPROACH TO TARGET LOCALIZATION

4.1 target localization with error-free TDOA measurements

The scenario of a target entering the surveillance zone of the passive detection system shown in Figure 2.1 will be used to examine target localization. A non-coplanar receiver configuration will be used in the investigation; it has better accuracy in estimating the target's altitude [15]. To see how TDOA measurement error affects target localization accuracy, it is helpful to first establish a reference case in which there are no errors in the TDOA measurements as reference so that comparison can be made with cases where errors are present. For this purposes, a set of 3 error-free TDOA measurement values (d_{ij}) are extracted from the scenario in Figure 2.1 as reference sets. Since the target's flight path (ground truth) and the receiver locations are known a-priori, error-free d_{ij} values can be calculated from Equation (2.1). Alternatively, error-free TDOA measurement values can be generated using very wide bandwidth signals and very high system SNR according to Equation (3.10).

As the target traverses through the surveillance zone, signals from the target are taken at 10 time intervals; these are shown as open circles in Figure 2.1a. TDOA-measurement values, d_{12} , d_{34}, d_{14} are calculated at each of the 10 time instants from each of the 3 receiver-pairs S1-S2, S3-S4 and S1-S4 respectively.
A set of 3 hyperboloids is then generated using Equation (2.5) at each of the 10 time instants along the target's flight path; target localizations are extracted from the intersection point of the 3 hyperboloid surfaces. The intersection point is determined by scanning along altitude z with an increment of 1 m for a range of altitude from z = 0 to 2000m (see Figure 2.5 for an illustration of 3 intersecting hyperboloids). At each altitude z, Equation (2.1) in the form of a residual quantity given by,

$$S = \sum_{k} | d_{ij} - (r_i - r_j) |_{k(i,j)} \quad (4.1)$$

is computed [24]. At the altitude z where S is closest to zero, that is where the point of intersection of the 3 hyperboloids is located, pinpointing the target location in x, y, z. That is, a minimum S is sought along the z-direction to pinpoint the intersection of the 3 hyperboloids. The subscript k is an index indicating the 3 receiver pairs (i,j) used in the TDOA measurements, e.g., $k(1,2) = 1$, $k(3,4) = 2$, $k(1,4) = 3$. A minimum S is equivalent to having a sharp intersecting point with the smallest area formed by the 3 intersecting hyperboloids at z.

Table 4.1 shows the computed target localization results (x,y,z) and the target ground truths (X_{Tg},Y_{Tg},Z_{Tg}) for comparison. The results indicate that the computed target locations are accurate to within 1m in altitude z, the increment size of the altitude scan; the computed (x,y) coordinates are identical to the ground truth values. Thus, for all practical intents and purposes, the computed results show that the 3 hyperboloids do intersection at a point when there is no error in the TDOA measurements d_{ij}, hence providing very accurate target localization in x, y, z.

Table 4.1: Comparisons of target localization from error-free TDOA measurements and target ground-truth positions.

	Target ground truth (m)			Computed target location (m)		
Time (arb.unit)\	X_{Tg}	Y_{Tg}	Z_{Tg}	x	y	z
1	-660.00	9998.50	1000.00	-660.00	9998.50	1000.00
2	-608.44	9328.48	1000.00	-608.44	9328.48	1000.00
3	-556.89	8658.46	1000.00	-556.89	8658.46	1000.00
4	-505.33	7988.44	1000.00	-505.33	7988.44	1000.00
5	-453.78	7318.42	1000.00	-453.78	7318.42	1000.00
6	-402.22	6648.40	1000.00	-402.22	6648.40	1000.00
7	-350.67	5978.38	1000.00	-350.67	5978.38	1000.00
8	-299.11	5308.36	1000.00	-299.11	5308.36	1000.00
9	-247.56	4638.34	1000.00	-247.56	4638.34	1000.00
10	-196.00	3968.32	1000.00	-196.00	3968.32	1000.00

4.2 Target localization using TDOA measurements with errors

Drones transmit signals over a large range of bandwidths, spanning from β = 1 to 20 MHz (telemetry to ultra-high-definition TV images), and the nominal target detection threshold SNR value of a RF-signal detection system is usually set at $(S/N)_T$ = 16 [17,25]. For signals with finite bandwidths and systems with moderate SNR, the TDOA measurements will have errors as described by the Cramer-Rao Lower Bound error in Equation (3.10).

Two cases with different amount of TDOA measurement errors are examined. The first case considers signals with a bandwidth β = 1 MHz and $(S/N)_T$ = 16, resulting in a TDOA measurement error ε = 30 m. In the second case, β = 20 MHz and $(S/N)_T$ = 16, giving an ε = 1.5 m. The computed target localization results for these 2 cases are shown in Tables 4.2 and 4.3 for CRLB error ε = 30 m and 1.5 m respectively.
It can be seen that in the results for the larger error case (ε =30 m) in Table 4.2, the computed target locations are off considerably from the target's ground truths, especially the target's altitude. When the error in the TDOA measurements is reduced to ε = 1.5 m in the second case, the accuracy of the computed target locations improved quite significantly as seen in Table 4.3.

Table 4.2: Comparisons of target localization from TDOA measurements with errors and actual target positions for non-coplanar receiver system. β = 1 MHz, $(S/N)_T$ =16.

	Target ground truth (m)			Computed target location (m)		
Time (arb.unit)\	X_{Tg}	Y_{Tg}	Z_{Tg}	*x*	*y*	*z*
1	-660.00	9998.50	1000.00	-637.86	9837.28	400
2	-608.44	9328.48	1000.00	-624.27	9398.05	1700
3	-556.89	8658.46	1000.00	-543.75	8603.23	600
4	-505.33	7988.44	1000.00	-490.12	7938.34	800
5	-453.78	7318.42	1000.00	-441.23	7277.22	900
6	-402.22	6648.40	1000.00	-394.97	6562.24	900
7	-350.67	5978.38	1000.00	-344.75	5947.75	1200
8	-299.11	5308.36	1000.00	-288.28	5238.35	400
9	-247.56	4638.34	1000.00	-254.61	4595.83	1300
10	-196.00	3968.32	1000.00	-204.42	3923.01	1500

Table 4.3: Comparisons of target localization from TDOA measurements with errors and actual target positions for non-coplanar receiver system. β = 20 MHz, $(S/N)_T$ =16.

	Target ground truth (m)			Computed target location (m)		
Time (arb.unit)\	X_{Tg}	Y_{Tg}	Z_{Tg}	*x*	*y*	*z*
1	-660.00	9998.50	1000.00	-658.36	9985.12	1000.00
2	-608.44	9328.48	1000.00	-607.37	9320.40	1000.00
3	-556.89	8658.46	1000.00	-556.09	8649.78	1000.00
4	-505.33	7988.44	1000.00	-504.86	7981.78	1000.00
5	-453.78	7318.42	1000.00	-452.51	7313.34	1000.00
6	-402.22	6648.40	1000.00	-401.72	6644.95	1000.00
7	-350.67	5978.38	1000.00	-349.92	5975.92	1000.00
8	-299.11	5308.36	1000.00	-298.84	5306.21	1000.00
9	-247.56	4638.34	1000.00	-247.41	4636.79	1000.00
10	-196.00	3968.32	1000.00	-195.37	3966.59	1000.00

5. MULTIPLE TARGETS LOCALIZATION

As small drones are becoming increasingly easier to access, it is expected that encounters with multiple targets will become common occurrence. For practical counter-measures against drone surveillance, a detection system must be able to detect and track multiple targets simultaneously. Moreover, not only multiple target detection is essential; the system must also be able to process the target information in real-time so that appropriate action can be taken immediately to address the security threats.

5.1 A case study for 7-target localization

A 7-target scenario is used to investigate multiple target localization using the geometric approach. Figure 5.1 shows the ground truths in x-y positions of the 7 targets inside the surveillance area of the detection system; all targets are cruising at an altitude of 1000 m. TDOA measurements are taken at 10 time instants for each target; these are represented by the open circles.

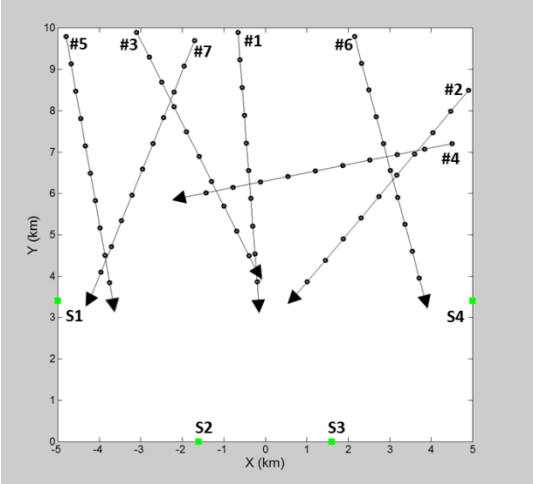

Figure 5.1: A 7-target scenario with multiple flight paths depicted in the monitored area; target positions at different time instants are given by the black circles and the positions of receivers S1, S2, S3, S4 are indicated by the green squares.

As in the case of the single target case, it requires 3 TDOA measurements (d_{12}, d_{34}, d_{14}), one from each of the 3 receiver pairs to localize a target. But in the 7-target case, each receiver pair will generate 7 TDOA measurement values corresponding to the 7 targets. Therefore, there will be 7^3 = 343 sets of possible combinations of 3 TDOA values in a permutation of all TDOA values. Among this large number of combinations, there are only 7 combinations that would provide the proper target locations. But all 343 combinations have to be analyzed to determine correct ones.

TDOA measurements with a CRLB error ε = 1.5 m are used to investigate the problem; this corresponds to using CRLB parametric values, β = 20 MHz, and $(S/N)_T$ = 16. Results of the computed target positions (x,y) indicated by the red diamonds are shown in Figure 5.2 and the corresponding computed target altitudes (z) are tabulated in Table 5.1. The computed target positions (x,y) for the most parts are quite accurate, except for a few occasions as marked by the black arrows showing the deviations in Figure 5.1.

The errors in locations from these occasions have been traced to the problem of finding the minimum S in a combination set of 3 TDOA measurement values from the permutation in which one of the TDOA values is belonging to a different target instead of the intended target [15]. The cause is thought to be related to the error size in the TDOA measurement values d_{ij}. To test and verify this conjecture, the error in the TDOA values d_{ij} is reduced by a factor of 10 to ε =0.15 m using β = 20 MHz, and $(S/N)_T$ = 1600 in the CRLB estimate in Equation (3.10). Figure 5.3 and Table 5.2 show the outputs of the target positions (x,y) and target altitudes (z) respectively. It is seen that all the computed target positions are placed correctly and at the correct target altitude. These results indicate that by reducing the TDOA measurement errors, localization of multiple targets can be processed accurately.

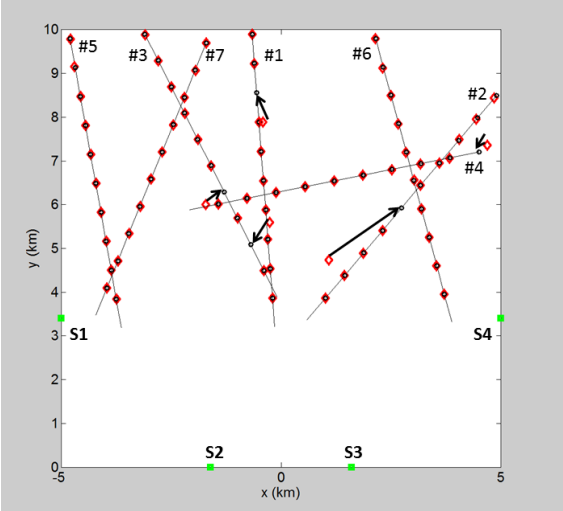

Figure 5.2: Computed target locations (x,y) from a non-coplanar configuration. CRLB: β = 20 MHz, $(S/N)_T$ = 12dB

Table 5.1: Computed target altitudes from a non-coplanar configuration. CRLB: β = 20 MHz, $(S/N)_T$ = 12 dB. Actual target altitude = 1000m.

	target altitude (m)						
	T#5	T#3	T#7	T#1	T#6	T#2	T#4
time							
1	1000.00	1000.00	1000.00	1000.00	1000.00	800.00	1600.00
2	1100.00	1000.00	1000.00	1000.00	900.00	900.00	1000.00
3	1000.00	1000.00	1000.00	700.00	1000.00	1000.00	1100.00
4	1000.00	1000.00	1000.00	1000.00	1000.00	1000.00	1000.00
5	1000.00	1000.00	1000.00	1000.00	1000.00	1000.00	1000.00
6	1000.00	1000.00	1000.00	1000.00	1000.00	1100.00	1700.00
7	1000.00	1000.00	600.00	1000.00	1000.00	1000.00	1000.00
8	1000.00	1000.00	1000.00	1000.00	1000.00	1000.00	1000.00
9	1000.00	1000.00	1000.00	800.00	1000.00	1000.00	1000.00
10	1000.00	1000.00	1000.00	1000.00	1000.00	1000.00	1000.00

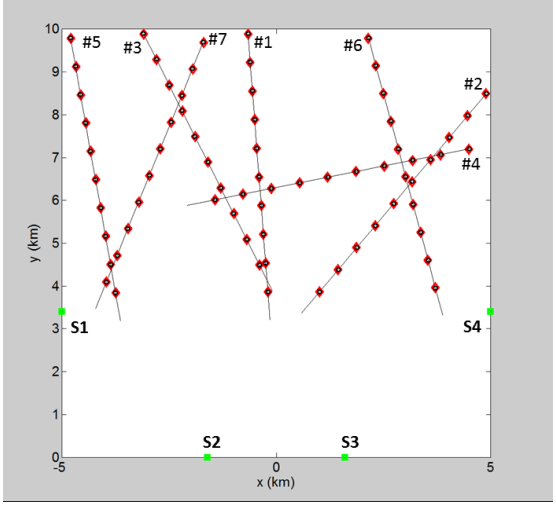

Figure 5.3: Computed target locations (x,y) from a non-coplanar configuration. β = 20 MHz, $(S/N)_T$ = 32dB.

Table 5.2: Computed target altitudes from a non-coplanar receiver configuration. β = 20 MHz, $(S/N)_T$ = 32dB. Actual target altitude = 1000 m.

	target altitude (m)						
	T#5	T#3	T#7	T#1	T#6	T#2	T#4
time							
1	1000.00	1000.00	1000.00	1000.00	1000.00	1000.00	1000.00
2	1000.00	1000.00	1000.00	1000.00	1000.00	1000.00	1000.00
3	1000.00	1000.00	1000.00	1000.00	1000.00	1000.00	1000.00
4	1000.00	1000.00	1000.00	1000.00	1000.00	1000.00	1000.00
5	1000.00	1000.00	1000.00	1000.00	1000.00	1000.00	1000.00
6	1000.00	1000.00	1000.00	1000.00	1000.00	1000.00	1000.00
7	1000.00	1000.00	1000.00	1000.00	1000.00	1000.00	1000.00
8	1000.00	1000.00	1000.00	1000.00	1000.00	1000.00	1000.00
9	1000.00	1000.00	1000.00	1000.00	1000.00	1000.00	1000.00
10	1000.00	1000.00	1000.00	1000.00	1000.00	1000.00	1000.00

5.2 Approach to real-time multi-target processing

For practical applications, a target detection system must be able to provide location information of multiple targets in real time so that the intruding targets can be dealt with immediately. One advantage of the geometric approach is that it may be able to facilitate real-time processing in multi-target scenarios. Using the geometry-based method, each of the 3 TDOA equations in equation (2.1) can be solved individually. A hyperboloid that corresponds to a given TDOA measurement value d_{ij} in each TDOA equation can be pre-computed. Look-up tables for a set of hyperboloids corresponding to a range of d_{ij} values can be generated. The look-up tables can speed up the target localization computing process, thus helping to facilitate real-time multiple targets processing.

For a given receiver system configuration, the receiver locations are a-priori information. Based on the separation distance d between a receiver pair Si-Sj, the range of the TDOA measurement values d_{ij} is between $-d < d_{ij} < d$ according to Equation (2.3). Furthermore, based on a given operating receiver bandwidth and detection SNR, the spacing of the d_{ij} values needed in generating the look-up tables can be determined from the Cramer-Rao Lower Bound error given in Equation (3.10).

Using a receiver system configuration as shown in Figure 2.1 as an example, a description on how a set of TDOA values can be determined for generating look-up tables of hyperboloids is given as follows. For receiver-pair S1-S2, the separation distance between receivers S1 and S2 is d = 4812m. For receiver operating with a bandwidth β = 20 MHz, and $(S/N)_T$ = 16, the set of TDOA values d_{12} will have a spacing of ε = 1.5 m as given by Equation (3.10). Thus a set of 6417 d_{12} values ($2d/\varepsilon$ + 1) are required in the look-up table for receiver-pair (S1-S2); i.e., d_{12} = 0, ±1.5, ±3, ⋯, ±4812. Similarly, it will require 6417 d_{34} TDOA values for receiver-pair S3-S4. For receiver-pair S1-S4, the distance separating S1 and S4 is d = 10000 m; therefore, $2d/\varepsilon$ + 1 = 13334 d_{14} TDOA values are required. A hyperboloid can be pre-computed for each of these TDOA values, totaling 26168 in all. This is very manageable in terms of storage requirement using current technology available.

For a n-target scenario, there are n^3 combinations of 3-hyperboloids from a permutation of n targets that have to be search to find the n-target localization. The pre-computed hyperboloids would save a significant amount of computing time. Processing of n^3 combinations using look-up tables can facilitate real-time (~ 1s) target localization to be realized for a reasonable size n.

Table 5.3 gives an indication of the amount of computing time used in processing TDOA measurements conducted in this study. The time taken includes the generation and orientation of the 3 hyperboloids as outlined in Section 2, and the search for minimum S in Equation (4.1) for n targets in a sequential permutation processing for each target. The computations are performed in a Dell T7400 workstation.

Table 5.3: Computation time consumed in target localization processing for different number of targets detected using sequential processing.

n (no. of targets detected)	t (computing time)
1	18.6s
3	56.1
7	147.1
10	236.0

The long computing time required for the non-coplanar configuration is due to resampling of the mesh of the hyperboloid in the z-direction so that all 3 hyperboloids have the same z-grid mesh to determine the target localization correctly. However, computing time requirement should no longer be an issue if the hyperboloids are pre-computed. Using look-up tables, efficient data-file search algorithms, parallel processing, faster multi-processor computer, and further streamlining and optimizing of the computational codes, it is conceivable that a 1-s target localization time can be realized for a 10-target scenario.

6.0 CONCLUSIONS

Passive target localization exploiting the target's emitting radio-frequency signals has been investigated. The TODA method is employed in the passive target localization process. A geometry-based approach to solving the set of TDOA equations has been proposed. Target location is then determined by searching for the intersection of the hyperboloid surfaces that represent the solutions to the TDOA equations. Target location accuracy is examined as a function of TDOA measurement errors. The errors are modelled using the Cramer-Rao Lower Bound to provide an estimate on how accurate the TDOA measurements can be made in the signal correlation process.

Numerical results from the analysis show that the geometric approach can provide accurate target localization. Localization of multiple targets using the geometry-based approach has also been examined. Results indicate that accurate multiple-target localization can be obtained; however, real-time processing may be a challenge. The geometric approach may offer a solution to reduce a significant portion of the processing time. It can be used in conjunction with pre-computed look-up tables of target hyperboloids to improve the processing speed. This opens up a potential means to real-time multi-target localization processing.

As drones become more affordable and accessible, multi-target threats are likely to become more likely to occur. A multi-target, real-time detection and tracking will likely be a desirable capability, and may become a standard requirement in a field system to handle practical drone counter-measures applications. This paper has proposed and examined an approach that could achieve such capability.

7.0 REFERENCES

[1] R.A. Poisel, “Electronic Warfare Target location Methods”, ArtTech House, Boston, 2005.
[2] D. Munoz, F. Bouchereau, C. Vargas, R. Enriquez-Caldera, “Position Location Techniques and Applications”, Academic Press, Burlington MA, 2009.
[3] J. P. Van Etten, “Navigation systems: Fundamentals of low- and very-low-frequency hyperbolic techniques”, Electrical Communication, Vol. 45, No. 3, pp.192-212, 1970.
[4] H. C. Schau and A. Z. Robinson, “passive sources localization employing intersecting spherical surfaces from time-of-arrival differences”, IEEE Transactions on Acoustics, Speech, and Signal Processing, Vol. ASSP-35, No.8 pp.1223-1225, August 1987.
[5] J. Abel and J. Chaffe, “Existence and uniqueness of GPS solutions”, IEEE Transactions on Aerospace and Electronic Systems, Vol. 27, No. 6, pp.952-956, November 1991.
[6] J. Bard, F. M. Ham, and W. L. Jones, “An algebraic solution to the time-difference of arrival equations”, Southeastcon ’96, Proceedings of the IEEE, pp.313-319, Tampa, FL, 11-14 Apr 1996.
[7] T. Sathyan, A. Sinha, and T. Kirubarajan, “Passive geolocation and tracking of an unknown number of emitters”, IEEE Transactions on Aerospace and Electronic Systems, Vol. 42, No.2, pp.740-750, April 2006.
[8] M. Wax and T. Kailath, “Optimum localization of multiple sources by passive arrays”, IEEE Transactions on Acoustics, Speech, and Signal Processing, Vol. ASSP-31, No.5 pp.1210-1217, October 1983.
[9] Y. T. Chan, and K. C. Ho, “A simple and efficient estimator for hyperbolic location”, IEEE Transactions on Signal Processing, Vol.42, No.8, pp.1905-1915, August 1994.
[10] G. Mellen, M. Pachter, and J. Raquet, “Closed-form solution for determining emitter location using time difference of arrival measurements”, IEEE Transactions on Aerospace and Electronic Systems, Vol. 39, No. 3, pp.1056-1058, July 2003.
[11] B. Fang, “Simple solution for hyperbolic and related position fixes”, IEEE Transactions on Aerospace and Electronic Systems, Vol. 26, No. 5, pp.748753, September 1990.
[12] F. C. Schweppe, “Sensor array data processing for multiple signal sources”, IEEE Transactions on Information Theory, Vol.IT-14, pp.294-305, February 1968.
[13] R. Schmidt, “Least squares range difference location”, IEEE Transactions on Aerospace and Electronic Systems, Vol. 32, No. 1, pp.234-242, January 1996.
[14] D. A. Brannan, M. F. Esplen and J. J. Grey, “Geometry”, Cambridge University Press, 1999.
[15] S. Wong, R. Jassemi, D. Brookes, and B. Kim, “Passive target localization using a geometric approach to the time-difference-of-arrival method”, Defence Research and Development Canada, Scientific Report, DRDC-RDDC-SR17, 2017.

[16] W. R. Hahn and S. A. Tretter, “Optimum processing for delay-vector estimation in passive signal arrays”, IEEE Transactions on Information Theory, Vol.IT-19, No.5, pp.608-614, September 1973.
[17] S. Stein, “Algorithms for ambiguity function processing”, IEEE Transactions on Acoustics, Speech, and Signal Processing, Vol. ASSP-29, No.3 pp.588-599, June 1981.
[18] C. H. Knapp and G. C. Carter, “The generalized correlation method for estimation of time delay”, IEEE Transactions on Acoustics, Speech, and Signal Processing, Vol. ASSP-24, No.4 pp.320-327, August 1976.
[19] ”Radar Handbook”, Editor, M. Skolnik, Second Edition, McGraw-Hill, 1990.
[20] D. R. Wehner, “High Resolution Radar”, Artech House, Boston, 1987.
[21] A.W. Rihaczek, “Principles of High Resoultion Radar”, Artech House, Boston, 1996.
[22] R. N. McDonough, and A. D. Whalen, “Detection of Signal in Noise”, Second Edition, Academic Press, 1995.
[23] A. H. Quazi, “An overview on the time delay estimation in active and passive systems for target localization”, IEEE Transactions on Acoustics, Speech, and Signal Processing, Vol. ASSP-29, No.3 pp.527-533, June 1981.
[24] J. O. Smith and J. S. Abel, “Closed-form least-square source location estimation from range-difference measurements”, IEEE Transactions on Acoustics, Speech, and Signal Processing, Vol. ASSP-35, No.12 pp.1661-1669, December 1987.
[25] S. Henriksen, “Unmanned Aircraft Control and ATC Communications Bandwidth Requirements”, NASA/CR-2008-214841, 2008.